Spin-glass state and long-range magnetic order in Pb(Fe$_{1/2}$Nb$_{1/2}$)O$_3$ seen via neutron scattering and muon spin rotation

G. M. Rotaru,[1] B. Roessli,[1] A. Amato,[2] S. N. Gvasaliya,[1] C. Mudry,[3] S. G. Lushnikov,[4] and T. A. Shaplygina[4]

[1]*Laboratory for Neutron Scattering, ETH Zurich and Paul Scherrer Institut, CH-5232 Villigen PSI, Switzerland*

[2]*Laboratory for Muon Spin Spectroscopy, Paul Scherrer Institut, CH-5232 Villigen PSI, Switzerland*

[3]*Condensed matter theory group, Paul Scherrer Institut, CH-5232 Villigen PSI, Switzerland*

[4]*Ioffe Physical Technical Institute, Russian Academy of Science, 26 Politekhnicheskaya, 194021 St. Petersburg, Russia*

(Received 13 January 2009; revised manuscript received 19 March 2009; published 28 May 2009)

We have investigated the magnetic ground state of the multiferroic relaxor ferroelectric Pb(Fe$_{1/2}$Nb$_{1/2}$)O$_3$ with μSR spectroscopy and neutron scattering. We find that a transition to a partially disordered phase occurs below $T=20$ K that coexists with long-range antiferromagnetic ordering. The disordered phase resembles a spin glass. No clustering of magnetic ions could be evidenced by μSR so that the coexistence appears homogeneous in the sample.

I. INTRODUCTION

Since the discovery of a large magnetoelectric effect in RMn$_2$O$_3$ (Ref. 1) and RMn$_2$O$_5$ (Ref. 2) (R=rare earth), there is a revival of interest in the study of multiferroic materials where the coupling between the electric polarization and the magnetic order is strong. Although coexistence of ferroelectricity and magnetic long-range order is not very common, quite a number of new multiferroics materials have been found recently, such as Ni$_3$V$_2$O$_8$,[3] MnWO$_4$,[4] or LiCuVO$_4$,[5] to cite only a few. Multiferroics that have coupled ferroelectric and magnetic order parameters are also promising materials for applications as it is possible to control the ferroelectric polarization by a magnetic field and vice versa.[6] Therefore, there is an extensive search for materials that show pronounced magnetoelectric effect at ambient conditions. B-site-disordered complex perovskites PbB$'_x$B$''_{1-x}$O$_3$ might be attractive candidates as they can adopt various ions which strongly influence the temperature of magnetic and ferroelectric orderings.

Lead iron niobate, Pb(Fe$_{1/2}$Nb$_{1/2}$)O$_3$ (PFN), is one of the well-known complex perovskites that exhibits multiferroic properties.[7] PFN is rhombohedral at room temperature and cubic above the ferroelectric Curie temperature of 383 K.[8] Pb(Fe$_{1/2}$Nb$_{1/2}$)O$_3$ undergoes a diffuse phase transition without pronounced frequency dispersion.[9] In the cubic phase, the symmetry of the chemical cell is $Pm\bar{3}m$. There is a cubic-tetragonal phase transition at $T=383$ K followed by a first-order transition at 354 K. The symmetry of the chemical structure of the low-temperature phase of PFN was the subject of some debate. Lampis *et al.*[10] reported that the structure is monoclinic with space group Cm, whereas Ivanov *et al.*[11] using powder neutron-diffraction data found that the chemical structure of Pb(Fe$_{1/2}$Nb$_{1/2}$)O$_3$ has $R3c$ symmetry at $T=10$ K.

The magnetic properties of PFN are also not completely understood. PFN undergoes a paramagnetic to antiferromagnetic phase transition at $T_N \sim 140-160$ K.[12] The magnetic structure was determined by single-crystal neutron diffraction and corresponds to a simple G-type antiferromagnetic arrangement of the magnetic moments at all temperature be-

low T_N.[13] Magnetoelectric effect in PFN at low temperatures has been demonstrated long ago[14] and, recently, it was shown that the dc magnetic susceptibility has an anomaly at the paraelectric-ferroelectric phase transition.[15] The dielectric permeability also shows an anomaly at the Néel temperature,[16] which suggests that a biquadratic term in the Landau free energy of the form P^2M^2 is responsible for the coupling between the ferroelectric polarization P and the (staggered) magnetization M. Additional magnetic anomalies were reported in the literature for Pb(Fe$_{1/2}$Nb$_{1/2}$)O$_3$ below the magnetic phase transition. Both NMR (Ref. 17) and susceptibility measurements[18] have shown that an additional magnetic phase transition occurs in PFN around $T_g \sim 20$ K that was interpreted as the formation of a spin-glass phase by Kumar *et al.*[19]

Here we report on muon-spin rotation and neutron scattering results of the magnetic properties of PFN below the Néel temperature. We show that the magnetic ground state of Pb(Fe$_{1/2}$Nb$_{1/2}$)O$_3$ is a spin-glass-like state that coexists with long-range antiferromagnetic order below $T_g \simeq 20$ K.

II. EXPERIMENTAL

The Pb(Fe$_{1/2}$Nb$_{1/2}$)O$_3$ single crystals used in the muon-spin rotation and neutron-scattering experiments were grown by spontaneous crystallization from the melt following the routine described in Ref. 19. The muon-spin-relaxation measurements were performed using the GPS instrument at the Paul Scherrer Institut (Villigen, Switzerland) on a Pb(Fe$_{1/2}$Nb$_{1/2}$)O$_3$ single crystal between 160 and 5 K. Data were recorded using the zero-field method that allows us to determine both the static and dynamics in disordered spins systems. The neutron-scattering experiments were performed with the cold neutron three-axis spectrometer TASP (Ref. 20) at neutron spallation source SINQ operated in diffraction mode at $k_f=1.97$ Å^{-1}. For this experiment a single crystal of Pb(Fe$_{1/2}$Nb$_{1/2}$)O$_3$ was oriented with the $[1,1,0]$ and $[0,0,1]$ crystallographic directions in the scattering plane. In that scattering geometry, magnetic Bragg peaks with indices $(h/2,h/2,l/2)$ in the rhombohedral setting can be accessed. The use of a three-axis spectrometer was justified by the

need to improve the intensity-to-background ratio in order to search for possible short-range order at low temperatures.

III. RESULTS

A. μSR

In a μSR experiment, the time evolution of the muon-spin polarization is monitored by recording the asymmetric emission of positrons produced by the weak decay of the muon (muon lifetime ~ 2.2 μs). The time histogram of the collected positrons is given by

$$N(t) = N_0 \exp(-t/\tau)[1 + AG_z(t)] + B, \qquad (1)$$

where A is the initial muon asymmetry parameter, N_0 is a normalization constant, and B is a time-independent background. The function $G_z(t)$ reflects the normalized muon-spin autocorrelation function

$$G_z(t) = \frac{\langle \vec{S}(t) \cdot \vec{S}(0) \rangle}{\vec{S}^2(0)}, \qquad (2)$$

where $\vec{S}$ is the spin of the muon. Hence $AG_z(t)$, often called the μSR signal, reflects the time evolution of the muon polarization.

Figure 1 shows the μSR signal in $Pb(Fe_{1/2}Nb_{1/2})O_3$ upon passing the Néel temperature. In the paramagnetic phase the signal is consistent with a weak depolarization of the muon signal solely due to nuclear dipole moments. Below the Néel temperature, the muon signal changes rapidly and the initial asymmetry A is strongly reduced. This indicates that there is a large distribution of internal fields seen by the μ^+, which is a consequence of the random distribution of the Fe and Nb ions in the chemical lattice. Therefore, the μSR signal is depolarized and the residual asymmetry is close to 1/3 of the value observed in the paramagnetic state. Hence, in the long-range antiferromagnetic phase, the muon signal reflects only muons having their initial polarization along the direction of the internal field at the stopping site.

Below T_N, the time evolution of the remaining μSR signal is best fitted assuming the function

$$G_z(t) = \frac{1}{3}\exp[-(\lambda t)^{\beta}]. \qquad (3)$$

Close to T_N, the power exponent is $\beta \simeq 1$, reflecting the presence of fluctuating internal magnetic fields with a unique correlation time τ_c. In this range of temperatures, the depolarization rate λ is proportional to the second moment of the magnetic-field distribution $\langle B^2 \rangle$ and to the correlation time τ_c of the internal field and is given by

$$\lambda = \gamma_\mu^2 \langle B^2 \rangle \tau_c, \qquad (4)$$

where γ_μ is the muon gyromagnetic ratio. The temperature dependence of the depolarization rate λ is shown in Fig. 2. It can be observed that there is a critical-like divergence close to $T_g = 20$ K. This is a clear evidence that $Pb(Fe_{1/2}Nb_{1/2})O_3$ undergoes a second magnetic phase transition at the temperature T_g.

Figure 3 depicts the temperature evolution of the β exponent. As already mentioned, at temperatures just below T_N,
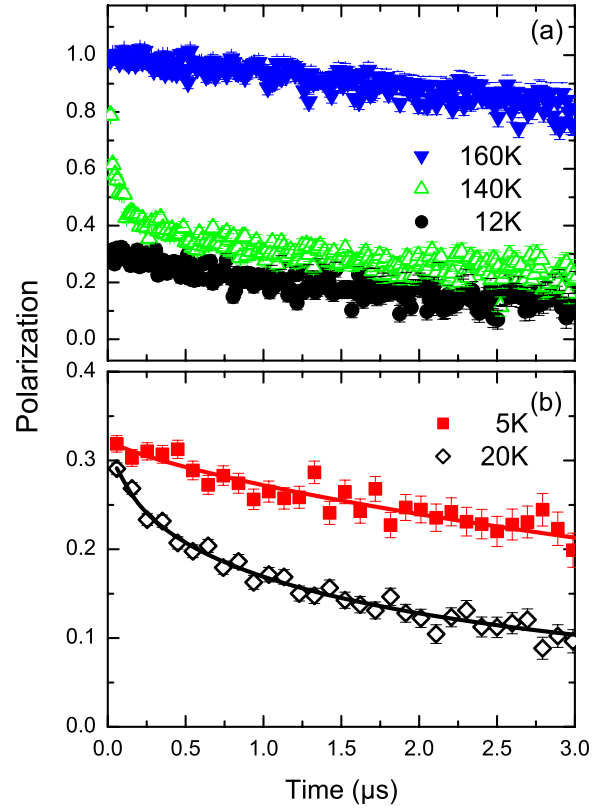

FIG. 1. (Color online) (a) Time evolution of the muon-spin polarization reported for characteristic temperatures. Note the weak depolarization in the paramagnetic phase (160 K) and the loss of the signal amplitude below T_N, which retains the value 1/3 ($t=0$) at low temperatures. (b) Examples of polarization signals recorded close to (20 K) and well below (5 K) T_g. The lines represent fits performed with Eq. (3) [data reported on (b) are strongly binned for clarity].

the muon depolarization is described by an exponential function instead of a stretched exponential, i.e., with the parameter $\beta \sim 1$. Upon further cooling below T_N, β continuously decreases and approaches the value of 1/3 at $T_g \sim 20$ K. A decrease in the exponent β toward the value of 1/3 has been predicted theoretically and later observed for the dense spin-glass systems AgMn and AuFe alloys.[21] It is tempting to
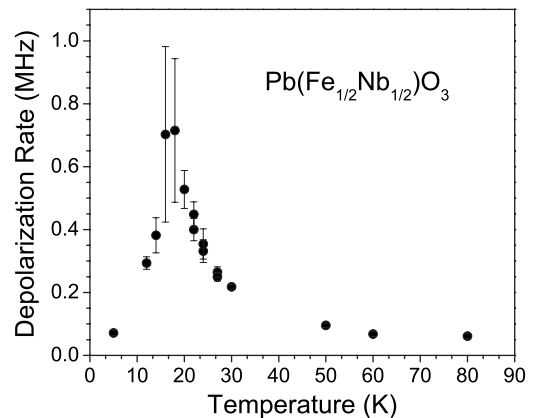

FIG. 2. Temperature dependence of the μSR depolarization rate λ below 80 K.
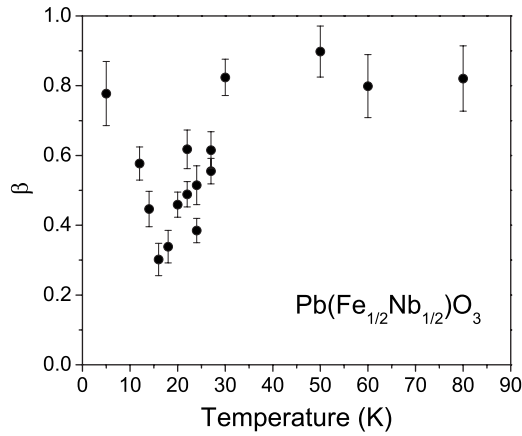
FIG. 3. Temperature dependence of the parameter β showing the occurrence of a distribution of relaxation times in PFN (see text).
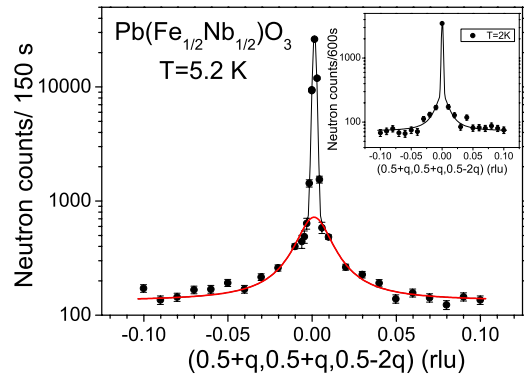

FIG. 4. (Color online) Transverse scans through the $\mathbf{Q}_N \equiv (0.5, 0.5, 0.5)$ magnetic Bragg peak. The broad component in the spectrum was fitted by a Lorentzian and is emphasized by a bold line. The Bragg peak is a fit to a Gaussian. Inset shows the intensity recorded in the neutron spin-flip channel for incident polarization along the scattering vector.

attribute this change in β to the change in the distribution of the correlation times τ_c of the internal magnetic fields at the muon stopping sites as a spin-glass transition is approached from above. However, for a usual paramagnetic to spin-glass transition, one observes that the residual fluctuations lead to a constant value of β below T_g while λ decreases, reflecting the decrease in the magnitude of the fluctuating field, as the temperature is lowered deeper into the spin-glass phase. However, Fig. 3 also shows that β grows as the temperature is lowered below T_g to recover the value ~ 1 at $T=2$ K. The solution to this apparent paradox is that the slow spin fluctuations, arising from the spin-glass state and which persist in a relatively broad temperature range below T_g, occur on top of antiferromagnetic fluctuations due to the long-range order. It is then natural to expect that the strong reduction in the critical spin-glass fluctuations in time when the temperature is decreased below T_g leads to the recovery of the weak noncritical antiferromagnetic fluctuations probed by the μSR signal above T_g. We note that as the static component of the μSR signal is already lost above T_g, no indication of a change (i.e., increase) in the damping of this component (as evidenced, for example, in other reentrant spin glasses[22]) could be determined at the spin-glass transition by μSR.

B. Neutron scattering

Figure 4 shows a typical neutron elastic scan along the $(q, q, -2q)$ direction at $T=5.2$ K in Pb(Fe$_{1/2}$Nb$_{1/2}$)O$_3$. The spectrum consists of a sharp Bragg peak centered around $\mathbf{Q}_N \equiv (1/2, 1/2, 1/2)$ that corresponds to the antiferromagnetic long-range order detected by neutron diffraction previously.[13] A diffuse component is also present in the neutron spectrum that is weaker in intensity and has a width in q that is much broader than the experimental resolution. The magnetic origin of the diffuse component was confirmed using the neutron polarization analysis device MuPAD (Ref. 23) that allows a complete separation of magnetic and nuclear scatterings. Namely, using a neutron-polarized beam for which the polarization is aligned along the scattering vector, magnetic scattering reverses the neutron polarization

vector, whereas scattering of nuclear origin leaves the polarization of the neutron beam unchanged. Magnetic scattering therefore appears in the spin-flip channel as shown to be the case for the diffuse component in the inset of Fig. 4.

We investigated the distribution of the diffuse scattering around the $\mathbf{Q}_N$ antiferromagnetic Bragg peak and found that it is essentially isotropically distributed in the $[1,1,0]/[0,0,1]$ scattering plane accessible in the present measurements (see Fig. 5). We performed an energy scan through the diffuse component and found that it is resolution limited within the energy window ($\Delta E = 0.3$ meV) of the spectrometer. Therefore, the spin fluctuations associated with the diffuse scattering are static in the time window of our experiment.

Within the quasistatic approximation, the energy-integrated neutron cross section is proportional to the generalized static susceptibility $\chi(\mathbf{Q})$,[24]
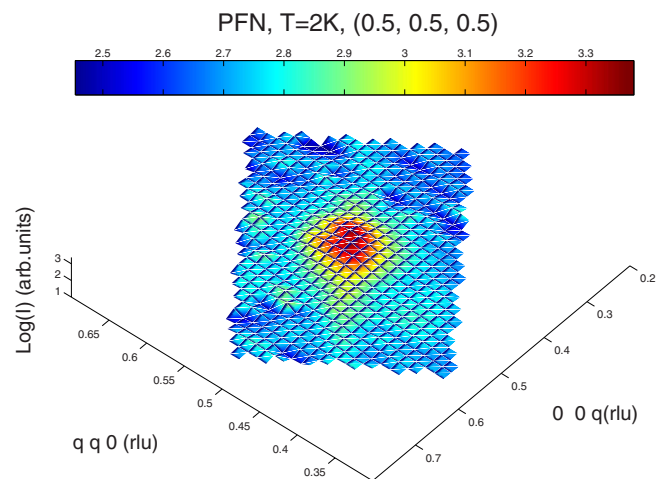

FIG. 5. (Color online) Distribution of the elastic diffuse scattering measured in Pb(Fe$_{1/2}$Nb$_{1/2}$)O$_3$ at $T=2$ K. For clarity the intense Bragg peak at $\mathbf{Q}_N \equiv (0.5, 0.5, 0.5)$ was removed and the background subtracted from the data.
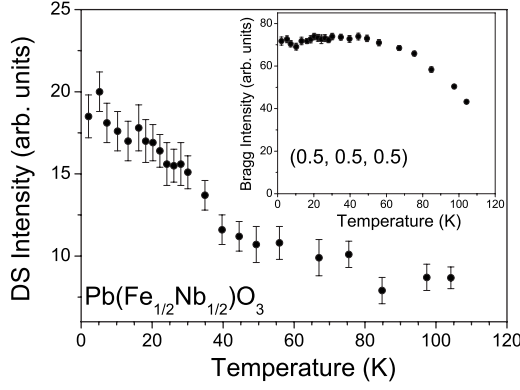
FIG. 6. Temperature dependence of the integrated intensity of the diffuse scattering in PFN measured around $\mathbf{Q}_N \equiv (0.5, 0.5, 0.5)$ Bragg peak. The temperature dependence of the antiferromagnetic Bragg peak is shown in the inset.

$$I(\mathbf{Q},T) \propto T \sum_{\alpha\beta} (\delta_{\alpha\beta} - \hat{\mathbf{Q}}_\alpha \hat{\mathbf{Q}}_\beta) \sum_{dd'} F_d(\mathbf{Q}) F_{d'}(\mathbf{Q}) \chi_{\alpha\beta}^{dd'}(\mathbf{Q})$$
$$\times \exp[i\mathbf{Q}(\mathbf{r}_d - \mathbf{r}'_d)]. \tag{5}$$

The term $(\delta_{\alpha\beta} - \hat{\mathbf{Q}}_\alpha \hat{\mathbf{Q}}_\beta)$ accounts for the fact that only fluctuations perpendicular to the scattering vector $\mathbf{Q}$ contribute to the diffuse intensity. The index d labels the spins at position $\mathbf{r}_d$ and $F_d(\mathbf{Q})$ is the magnetic form factor. We modeled the diffuse scattering measured along $(q, q, -2q)$ around the $\mathbf{Q}_N$ magnetic Bragg peak by a Lorentzian function

$$I(\mathbf{Q},T) = \frac{A(T)}{\kappa^2 + |\mathbf{Q} - \mathbf{Q}_N|^2}, \tag{6}$$

where $A(T)$ is the scattered intensity and $\kappa = 1/\xi$ is the inverse of the correlation length. The temperature dependence of the diffuse scattering intensity is shown in Fig. 6. Above $T \sim 120$ K the diffuse scattering is too weak to be separated from the background scattering. Below that temperature $A(T)$ increases monotonically with cooling down to $T \sim 2$ K. A fit to the neutron data with Eq. (6) yielded at all temperatures, for which the diffuse scattering could be observed, $\kappa \sim 0.015$ (rlu) that corresponds to $\xi \sim 17$ Å.

IV. CONCLUSION AND DISCUSSION

Both μSR spectroscopy and neutron diffraction have shown that a transition to a spin-glass state that coexists with long-range antiferromagnetic order occurs in the relaxor perovskite Pb(Fe$_{1/2}$Nb$_{1/2}$)O$_3$ at $T_g \simeq 20$ K. Figure 1 shows that the asymmetry of the muon signal is rapidly lost below T_N and does not recover when passing the spin-glass transition. This indicates that the magnetic order is homogeneous and that it persists upon cooling the sample below T_g. This is confirmed by the presence of the resolution-limited magnetic Bragg peak at the lowest temperature showing that long-range antiferromagnetic order of the Fe^{3+} spins is still present below T_g. The long-range antiferromagnetic order coexists with the disordered spin-glass-like phase. The signature of the spin-glass order appears in the neutron spectrum in the form of diffuse scattering.

There are numerous examples of coexistence between the ferromagnetic and spin-glass states of matter.[25] For example, ferromagnetic and spin-glass orders are known to coexist in AuFe alloys at sufficiently low temperatures.[26] Antiferromagnetic and spin-glass orders are also known to coexist at sufficiently low temperatures, e.g., in Fe$_{0.55}$Mg$_{0.45}$Cl$_2$.[27] The coexistence of collinear magnetic long-range order, e.g., ferromagnetic or antiferromagnetic, and spin-glass order is well understood theoretically at the level of the Sherrington-Kirkpatrick (SK) (Ref. 28) infinite-range model for classical (Ising or Heisenberg) spins. In the SK model, this coexistence is the rule below some critical temperatures and down to the lowest temperatures as soon as the magnitude $|\bar{J}|$ of the mean value of the random exchange coupling J between any two spins is on the order of or larger than the standard deviation ΔJ of its Gaussian distribution.[29–32]

Classical spin models with short range but random two-body spin interactions [the Edwards-Anderson (EA) model of spin glasses[33]] are not as well understood as the SK model. Monte Carlo simulations suggest that the lower-critical dimension for the onset of spin-glass order when the disorder is dominant, $|\bar{J}|/\Delta J \ll 1$, is strictly below three dimensions for Ising spins,[34] a prerequisite for the coexistence of collinear and spin-glass order when $|\bar{J}|/\Delta J \gtrsim 1$.[35] Fluctuation effects are stronger for Heisenberg spins than they are for Ising spins, as fluctuations in the directions transverse to the direction taken by the collinear order parameter in spin space become available in the former case. Correspondingly, state-of-the-art Monte Carlo simulations give "only" the upper bound of three dimensions for the spin-glass lower-critical dimension when the disorder is dominant, $|\bar{J}|/\Delta J \ll 1$.[36] In other words, it cannot be ruled out within the accuracy of available Monte Carlo simulations that the spin-glass phase is quasi-long-range ordered instead of long-range ordered when the classical spins are Heisenberg type in the three-dimensional EA model.

Given the uncertainty of the spin-glass lower-critical dimension for Heisenberg EA spin-glass models, the mere observation that antiferromagnetic and spin-glass orders coexists in Pb(Fe$_{1/2}$Nb$_{1/2}$)O$_3$ is not sufficient to establish whether the relevant magnetic degrees of freedom are Ising or Heisenberg type. Although exchange interactions remain to be determined in Pb(Fe$_{1/2}$Nb$_{1/2}$)O$_3$, the relatively high Néel temperature of Pb(Fe$_{1/2}$Nb$_{1/2}$)O$_3$ suggests that exchange interactions dominate dipolar and single-ion anisotropies in this compound. If this is the case, then Pb(Fe$_{1/2}$Nb$_{1/2}$)O$_3$ is a good candidate to study the coexistence of long-range antiferromagnetic and spin-glass orders for the Heisenberg spins of a three-dimensional antiferromagnetic EA model.

[1] T. Kimura, T. Goto, H. Shintani, K. Ishizaka, T. Arima, and Y. Tokura, Nature (London) **426**, 55 (2003).

[2] N. Hur, S. Park, P. A. Sharma, J. S. Ahn, S. Guha, and S.-W. Cheong, Nature (London) **429**, 392 (2004).

[3] G. Lawes, M. Kenzelmann, N. Rogado, K. H. Kim, G. A. Jorge, R. J. Cava, A. Aharony, O. Entin-Wohlman, A. B. Harris, T. Yildirim, Q. Z. Huang, S. Park, C. Broholm, and A. P. Ramirez, Phys. Rev. Lett. **93**, 247201 (2004).

[4] K. Taniguchi, N. Abe, T. Takenobu, Y. Iwasa, and T. Arima, Phys. Rev. Lett. **97**, 097203 (2006).

[5] F. Schrettle, S. Krohns, P. Lunkenheimer, J. Hemberger, N. Büttgen, H.-A. Krug von Nidda, A. V. Prokofiev, and A. Loidl, Phys. Rev. B **77**, 144101 (2008).

[6] R. Ramesh and N. A. Spaldin, Nature Mater. **6**, 21 (2007).

[7] H. Schmid, in *Magnetoelectric Interaction Phenomena in Crystals*, edited by A. J. Freeman and H. Schmid (Gordon and Breach, New York, 1975).

[8] Y. Yokomizo, T. Takahashi, and S. Nomura, J. Phys. Soc. Jpn. **28**, 1278 (1970).

[9] M. V. Radhika Rao and A. M. Umarji, Mater. Res. Bull. **30**, 1031 (1995).

[10] N. Lampis, P. Sciau, and A. G. Lehmann, J. Phys.: Condens. Matter **11**, 3489 (1999).

[11] Sergey A. Ivanov, Roland Tellgren, Häkan Rundlof, Noel W. Thomas, and Supon Ananta, J. Phys.: Condens. Matter **12**, 2393 (2000).

[12] V. A. Bokov, I. E. Mylnikova, and G. A. Smolenskii, Zh. Eksp. Teor. Fiz. **42**, 643 (1961) [Sov. Phys. JETP **15**, 447 (1962)].

[13] B. Howes, M. Pelizzone, P. Fischer, C. Tabares-Munoz, J.-P. Rivera, and H. Schmid, Ferroelectrics **54**, 317 (1984).

[14] T. Watanabe and K. Kohn, Phase Transitions **15**, 57 (1989).

[15] R. Blinc, M. Kosec, J. Holc, Z. Trontelj, Z. Jaglicic, and N. Dalal, Ferroelectrics **349**, 16 (2007).

[16] Y. Yang, J.-M. Liu, H. B. Huang, W. Q. Zou, P. Bao, and Z. G. Liu, Phys. Rev. B **70**, 132101 (2004).

[17] R. Blinc, V. V. Laguta, B. Zalar, B. Zupancic, and M. Itoh, J. Appl. Phys. **104**, 084105 (2008).

[18] V. V. Bhat, K. V. Ramanujachary, S. E. Lofland, and A. M. Umarji, J. Magn. Magn. Mater. **280**, 221 (2004).

[19] A. Kumar, R. S. Katiyar, C. Rinaldi, S. G. Lushnikov, and T. A. Shaplygina, Appl. Phys. Lett. **93**, 232902 (2008).

[20] F. Semadeni, B. Roessli, and P. Boni, Physica B **297**, 152 (2001).

[21] I. A. Campbell, A. Amato, F. N. Gygax, D. Herlach, A. Schenck, R. Cywinski, and S. H. Kilcoyne, Phys. Rev. Lett. **72**, 1291 (1994).

[22] See, for example, I. Mirebeau, M. Hennion, M. J. P. Gingras, A. Keren, K. Kojima, M. Larkin, G. M. Luke, B. Nachumi, W. D. Wu, Y. J. Uemura, I. A. Campbell, and G. D. Morris, Hyperfine Interact. **104**, 343 (1997).

[23] M. Janoschek, S. Klimko, R. Gähler, B. Roessli, and P. Böni, Physica B **397**, 125 (2007).

[24] P. G. de Gennes and J. Villain, J. Phys. Chem. Solids **13**, 10 (1960).

[25] K. H. Fischer and J. A. Hertz, *Spin Glasses* (Cambridge University Press, Cambridge, England, 1991).

[26] A. P. Murani, Solid State Commun. **34**, 705 (1980); Phys. Rev. B **28**, 432 (1983).

[27] P. Z. Wong, S. von Molnar, T. T. M. Palstra, J. A. Mydosh, H. Yoshizawa, S. M. Shapiro, and A. Ito, Phys. Rev. Lett. **55**, 2043 (1985).

[28] D. Sherrington and S. Kirkpatrick, Phys. Rev. Lett. **35**, 1792 (1975).

[29] M. Gabay and G. Toulouse, Phys. Rev. Lett. **47**, 201 (1981).

[30] I. Ya. Korenblit and E. F. Shender, Sov. Phys. JETP **62**, 1030 (1985).

[31] Ya. V. Fyodorov, I. Ya. Korenblit, and E. F. Shender, J. Phys. C **20**, 1835 (1987).

[32] D. B. Liarte and C. S. O. Yokoi, J. Phys. A **41**, 324010 (2008).

[33] S. F. Edwards and P. W. Anderson, J. Phys. F: Met. Phys. **5**, 965 (1975).

[34] H. G. Ballesteros, A. Cruz, L. A. Fernandez, V. Martin-Mayor, J. Pech, J. J. Ruiz-Lorenzo, A. Tarancon, P. Tellez, C. L. Ullod, and C. Ungil, Phys. Rev. B **62**, 14237 (2000).

[35] A. D. Beath and D. H. Ryan, Phys. Rev. B **76**, 064410 (2007).

[36] For a recent review, see A. P. Young, J. Phys.: Conf. Ser. **95**, 012003 (2008).